



# Rebar Detection and Localization for Non-destructive Infrastructure Evaluation of Bridges Using Deep Residual Networks

Habib Ahmed<sup>1</sup>, Hung Manh La<sup>1(✉)</sup>, and Gokhan Pekcan<sup>2</sup>

<sup>1</sup> Advanced Robotics and Automation Lab, Department of Computer Science and Engineering, University of Nevada, Reno, NV 89557, USA

hahmed@nevada.unr.edu, hla@unr.edu

<sup>2</sup> Department of Civil and Environmental Engineering, University of Nevada, Reno, NV 89557, USA

**Abstract.** Nondestructive Evaluation (NDE) of civil infrastructure has been an active area of research for the past few decades. Traditional inspection of civil infrastructure, mostly relying on visual inspection is time-consuming, labor-intensive and often provides subjective and erroneous results. To facilitate this process, different sensors for data collection and techniques for data analyses have been used to effectively carry out this task in an automated manner. The purpose of this research is to provide a novel Deep Learning-based method for detection of steel rebars in reinforced concrete bridge elements using data from Ground Penetrating Radar (GPR). At the same time, a novel technique is proposed for the localization of rebar in B-scan images. In order to examine the performance of the rebar detection and localization system, results are outlined to demonstrate the feasibility of the proposed system within relevant practical applications.

**Keywords:** Structural Health Monitoring (SHM) · Non-Destructive Evaluation (NDE) · Ground Penetrating Radar (GPR) sensor · Convolutional Neural Networks (CNNs) · Deep Residual Networks (ResNets)

## 1 Introduction

The monitoring, maintenance and rehabilitation of critical civil infrastructure during their life-cycle is of paramount importance. Of the different components of civil infrastructure, the need for periodic assessment, evaluation and maintenance of highway bridges has been emphasized by studies in the recent past [1–4]. According to the National Bridge Inventory (NBI), there are more than 600,000 bridges in the United States [5]. Although, the number of marginally or seriously damaged bridges has been declining over the past few decades, the recent statistics provided by the US Department of Transportation have classified around 67,000 bridges as structurally deficient and 85,000 as functionally obsolete [5]. For many decades, health and status assessment of these structures have been performed primarily through visual inspection using human inspectors. While this approach remains essential for system health assessment, it presents significant limitations that hinder the detection of various defect types and

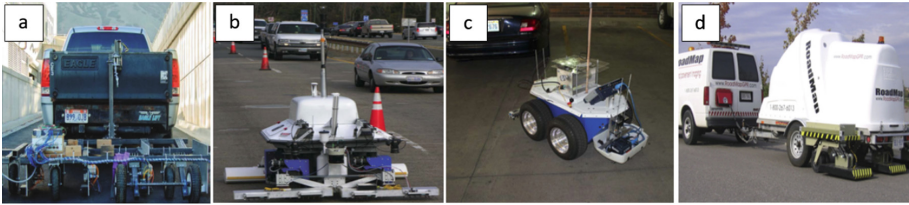


**Fig. 1.** State-of-the-art robotic platforms employing a wide-range of sensors for infrastructural monitoring, such as: (a) 7 channel impact-echo apparatus [15], (b) RABIT platform [12] (c) Seekur Jr. robotic platform [9], and (d) Roadmap system [10]

extent of damage that may lead to undesired consequences. In addition to other types of structural health monitoring (SHM) methods, non-destructive evaluation (NDE) techniques have the potential to streamline various forms of periodic inspections and to minimize the direct and indirect costs associated with failure of aging bridges. Therefore, the timely evaluation, monitoring and rehabilitation of bridges can reduce the overall direct as well as indirect costs and prevent loss of lives due to a possible structural failure and collapse.

This paper is presented in five sections. First, the motivation towards furthering the existing state-of-the-art for bridge deck evaluation and maintenance is discussed. Section 2 is dedicated to the discussion related to existing research conducted in the field of civil infrastructure assessment and evaluation. Section 3 presents the development of the proposed Deep Learning-based methodology for rebar detection and localization. Section 4 demonstrates the performance of the proposed approach. Finally, the overall conclusions are drawn and recommendations for future research has been provided in Sect. 5.

## 2 Related Works

Structural health monitoring (SHM) of civil infrastructure by means of NDE techniques has been a growing research area of interest in the recent past. Some of the major emerging themes in recent studies can be classified into research related to technological platforms, sensors and instrumentation modules for data collection, and algorithms for data analyses. Traditionally, tasks related to NDE have been performed visually by trained personnel [6]. However, in recent years, robotic platforms are being leveraged for infrastructure evaluation to enhance the overall efficiency and reduce the time-consumption and error in data collection. The usage of bridge-climbing robot for monitoring the condition of steel bridges was also proposed in a previous research [7]. An underwater robotic platform has been developed to monitor the condition of bridge piers [8]. Similarly, for the case of bridge evaluation, Gibb et al. [9] discussed the feasibility of a multi-functional, multi-sensor-based mobile platform containing GPR, electrical resistivity (ER) probe, and vision sensors. Figure 1(c) highlights the proposed robotic platform taking samples from an underground garage. Diamanti and Redman [10] used data from GPR sensors to examine surface and subsurface layer cracks using a ground-coupled Roadmap system, which has been outlined in Fig. 1(d). However, the

*Roadmap* platform cannot be considered as a truly robotic platform, as it requires manual assistance in terms of towing and driving with the help of a human driver.

Another novel robotic platform, namely the Robotics Assisted Bridge Inspection Tool (RABIT) has been designed for efficient automated evaluation of bridge decks [11–14]. This particular robotic platform has been equipped with different sensor technologies (e.g. impact echo, ultrasonic surface waves, electrical resistivity and GPR), which enable the classification of some of the most common defects in bridge decks, such as concrete degradation, delamination and rebar corrosion [11, 12]. Figure 1(b) shows the *RABIT* platform during the actual inspection and evaluation of a bridge deck. Its application and functionality have been further developed by La et al. [6] towards the automated monitoring of civil infrastructure using on-surface crack detection and bridge evaluation. In another recent research, a novel re-configurable platform spanning a maximum length of 12-ft was deployed that used seven channel impact-echo apparatus for infrastructure evaluation [15]. Figure 1(a) outlines the utilization of the re-configurable multi-channel impact-echo-based infrastructure evaluation platform towed at the back of human-operated vehicle.

The usage of GPR data for infrastructure evaluation has been in practice for as far back as the 1970s with applications that include void space detection, depth of concrete cover on bridges, locating metallic objects in concrete spaces, and general inspection and maintenance of reinforced concrete structures [16]. Some of the earlier studies have used GPR data for underground pipe detection [17], detection of underground objects, e.g. landmines and pipes [8], and examining defects in tunnels [18]. It is only recently that the shift has focused towards using GPR for bridge evaluation with particular emphasis on rebar detection and localization [12, 16, 19–23]. In the following discussion, the emphasis will be towards discussing the salient features of the proposed rebar detection and localization system. The rationale for using Deep Residual Networks for rebar detection will also be provided in view of the state-of-the-art in relevant research area.

### 3 System Methodology

In this section, a comprehensive evaluation of the different elements within the proposed method for rebar detection and localization will be highlighted. Earlier studies focusing on rebar detection and classification have used a number of different methods, ranging from Support Vector Machines [12] and Naïve Bayesian classifier [19] to the use of primitive Neural networks in some of the early studies using GPR for non-destructive infrastructure evaluation [8, 17]. One of the recent studies by Dinh et al. [24] has utilized a convolutional neural network for rebar detection. From a machine learning perspective, the detection and recognition of rebar from other non-rebar anomalies and artifacts detected in B-scans can be considered as a two-class classification problem. Earlier studies employing Residual Networks and their variants have attested to their superior performance towards tackling a vast range of research problems [25–27]. To the knowledge of the authors, there is no published work, which provides evaluation of Deep Residual Networks (ResNet-50) towards rebar detection and localization. It is for this reason that the present study employs one of the variants of the Deep Residual Networks

(i.e. ResNet-50) [28] as a critical sub-component of the overall system for rebar detection and localization. A preliminary analysis has been discussed in one of the recent works by the authors [20]. The present study is essentially a continuation and in-depth evaluation of the performance of Deep Residual Networks, along with its various pros and cons for the application towards NDE of bridges. Figure 2 depicts some of the salient features of the proposed system for rebar detection and localization.

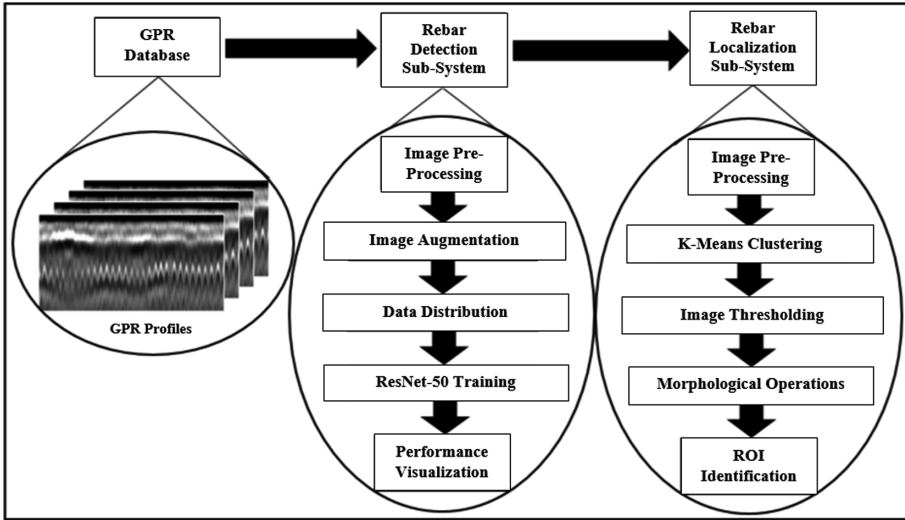


Fig. 2. Proposed system for rebar detection and localization

### 3.1 Proposed Model for Rebar Detection and Localization

Figure 2 outlines some of the basic building blocks for the rebar detection and rebar localization sub-systems. The first block of the proposed model is the GPR database, which leverages B-Scan data from different bridges to separate data for the two classes (i.e. rebar and non-rebar classes). The statistical information regarding the data and its distribution for testing and validation will be highlighted in the proceeding sections. Figure 3 provides details regarding the basic building block for ResNet-50. For system training using Deep Residual Network architecture (i.e. ResNet-50), a number of different operations have been performed, which include *image pre-processing* (different image operations are performed to reduce image noise and de-blurring), *image augmentation* (different transformation functions are applied to each image, which increases the dataset size and system performance), *data distribution* (random distribution of data into training and validation sets), *ResNet-50 model training* (use of data set for model training and validation to assess the performance of the rebar classification system) and *performance evaluation and visualization* (different performance measures are used to evaluate and visualize the system performance). Table 1 can be used to examine the different layers of the underlying network architecture for ResNet-50 used in this study.

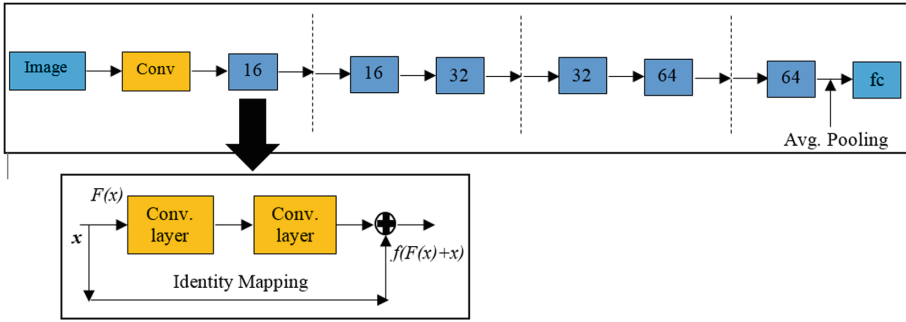


Fig. 3. Basic building block used for the development of Deep Residual Networks [28].

Table 1. Different properties of the Residual Network (ResNet-50) architecture [28]

Layer name	Input blocks	Output size
Conv1	$7 \times 7, 64, \text{stride } 2$	$112 \times 112$
Conv2	$3 \times 3 \text{ max pool, stride } 2$ $[1 \times 1, 64 \ 3 \times 3, 128 \ 1 \times 1, 512]$	$56 \times 56$
Conv3	$[1 \times 1, 128 \ 3 \times 3, 128 \ 1 \times 1, 512]$	$28 \times 28$
Conv4	$[1 \times 1, 256 \ 3 \times 3, 256 \ 1 \times 1, 1024]$	$14 \times 14$
Conv5	$[1 \times 1, 512 \ 3 \times 3, 512 \ 1 \times 1, 2048]$	$7 \times 7$
	Average pool, 1000-d fc Softmax	$1 \times 1$

With regard to the overall system for rebar detection and localization, it is important to understand that there is a sequential order between the consecutive blocks. This means that before the data is available to the different processes in the rebar localization sub-system, the data undergoes processing through the different functions outlined in rebar detection sub-system, which are given in Fig. 2. Once the rebar detection sub-system is able to differentiate between the rebar and non-rebar images, the images belonging to the former category are acquired by rebar localization sub-system to establish the physical presence of rebar artefact within the available data. Similar to the rebar detection sub-system, image pre-processing functions are used in the rebar localization sub-system to sharpen the intricate details and enhance the overall boundary between the background and parabolic artefact outlining the presence of underground steel rebars. K-means clustering algorithm [29] is used to segment the *background* (image pixels that do not contain rebar artefact information) and *foreground* (pixels that contain information related to rebar artefacts) information. In order to extract relevant information, the Image Thresholding technique has been used, which leads to the binarization of the original RGB image, along with some non-rebar artefacts [30]. In order to separate noise from rebar artefacts, a number of different morphological operations are utilized, namely morphological opening and closing operations [30]. Finally, the Region-of-Interest (ROI) is highlighted using the bounding box approach. The proceeding section will discuss some of the important findings in relation to the performance of the overall rebar detection and localization system.

## 4 Results and Discussion

### 4.1 Dataset

For the development of the proposed system for rebar detection and localization, GPR data has been acquired from a number of different sources. The dataset 1 has been acquired from a bridge located in Warren County, NJ, which was included as part of the data in one of the earlier studies [15]. Table 2 summarizes the dataset sizes for the different dataset used and their distribution between the training and validation phases for the two classes. To the knowledge of the authors, this dataset is the only publicly-available data of bridge inspection using GPR sensors. Dataset 2 is one segment of the overall GPR data collected from the inspection and evaluation performed on 40 different bridges in the United States between the time period of 2013 and 2014 [6, 11]. A portion of the available GPR data has also been used in a previous study [6, 18]. Since, dataset 2 contains GPR data from five different bridges, the overall number of images is considerably higher in comparison to dataset 1. Furthermore, the two datasets used in this study allow demonstration of the effect of data sizes on the system training as discussed in subsequent sections.

**Table 2.** Data set sizes used for training and validation

Name	Class rebar		Class no rebar		Total
	Training	Validation	Training	Validation	
Dataset 1	1,200	300	2,400	600	4,500
Dataset 2	1,043	228	7,027	2,040	10,338
Total	2,243	528	9,427	2,640	14,838

### 4.2 Rebar Detection Sub-system

In this section, the results obtained during the training and validation of the proposed system are presented. One of the most important system characteristics is the trained system accuracy, which is shown in Figs. 4 and 6 for dataset 1 and 2 respectively. In these figures, it can be seen that for the case of systems trained for different batch sizes, the overall system accuracy converges when the system is trained for 20 epochs, which means that training beyond this point does not result in significant gains in system performance. When examining Figs. 4 and 6 collectively it is important to realize that the y-axis scales vary for both these figures. In general, systems trained for higher epochs have higher accuracy than system trained for lower epochs. Figures 5 and 7 demonstrate the overall trend between number of epoch and time (in seconds) for the different values specified for batch size during training of the proposed system using dataset 1 and 2 respectively. From Fig. 5, it can be seen that when comparing the time taken for successful training of systems with different batch sizes, the batch size with the highest overall training time is 4. This shows that in order to optimize the training of the proposed system, a high level of batch size should be preferred. In order to fully

appreciate the scale of improvement in computational performance of the proposed system, Fig. 3 shows that the time necessary for training with batch size of 32 and 16 epochs is comparable to the training time for batch size of 4 and 8 epochs.

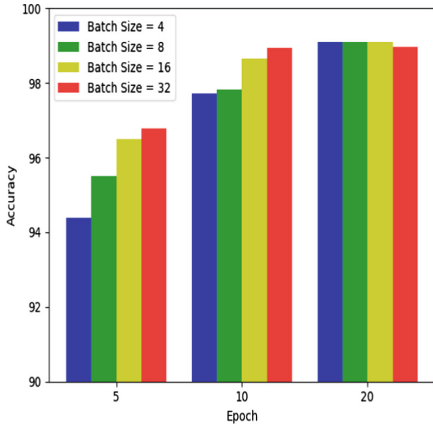


Fig. 4. Relationship between number of epochs and system accuracy for dataset 1.

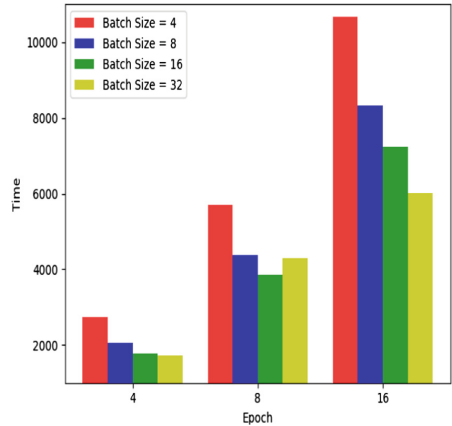
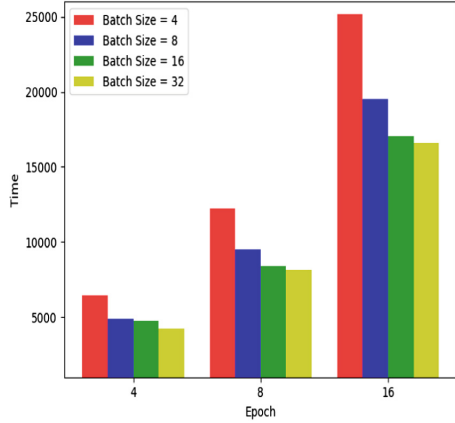
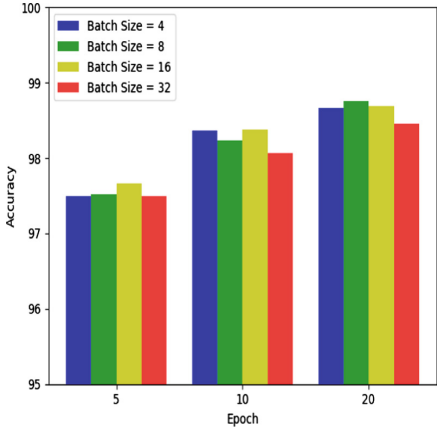


Fig. 5. Relationship between number of epochs and training time for dataset 1.

In this regard, Fig. 6 presents the results of system training for dataset 2 in terms of accuracy with increase in batch size and epochs for a specific range of values chosen for different system parameters. In contrast to the results obtained for dataset 1, it can be seen that the overall improvement in accuracy with increase in number of epochs is not pronounced for dataset 2. Similarly, it can be seen in Fig. 6, that increase in batch size does not necessarily result in considerably higher performance, specifically for the case of dataset 2. At the same time, there is very small variation in accuracy for the systems trained with different batch sizes. Furthermore, the results obtained for the case of batch size of 32 do not correspond to the highest performance. Due to the increased size of dataset 2, the training time is much higher in comparison to dataset 1, as highlighted in Fig. 5, which shows that system trained with smaller batch sizes undergo higher increase in training time. In general, for the training of the rebar detection sub-system, the inverse relationship between batch size and training time is evident, i.e. increase in batch size reduces the overall time taken for system training. In order to fully benefit from the magnitude of available GPR data, both dataset 1 and 2 had been concatenated. It has been examined in the relevant studies that the performance of Deep Learning-based algorithms is highly dependent on the scale of dataset being used for the system training [28].

Table 3 outlines the overall performance of the system trained using data from different dataset. It can be seen that the system trained after concatenation of the dataset 1 and 2 lead to the highest accuracy and lowest system loss metrics. However, in contrast to the training of dataset 1 and 2 separately, which were trained for 20 epochs each, the system utilizing both dataset 1 and 2 had to be trained for 100 epochs. It can be seen in Table 3 that the training time for system trained on the total data has the



**Fig. 6.** Relationship between number of epochs and system accuracy for dataset 2.

**Fig. 7.** Relationship between number of epochs and training time for dataset 2.

highest training time. The learning rate for all of the instances of system training was 0.005, which allowed for steady convergence with reduced probability of overfitting. The size of images in the dataset 1 and 2 had been fixed to  $81 \times 81$  pixels. The system used for performing the different computations had the following specifications: *Intel®* i5 processor with 2.3 GHz clock speed, 4 GB RAM, and 500 GB hard disk. In comparison with relevant studies [12, 19, 23, 24], the results highlighted in this research provide the highest system-level performance for rebar detection system. In the following sub-section, some of the relevant results and associated discussion regarding rebar localization sub-system will be provided.

**Table 3.** Summary of results for the Rebar Detection System trained using different dataset

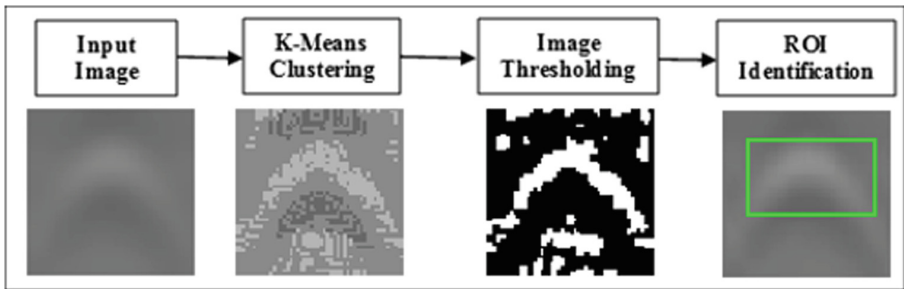
Dataset	System performance		
	Accuracy	System loss	Training time
Dataset 1	99.11%	2.91%	7,229 s
Dataset 2	98.75%	3.73%	17,067 s
Total	99.42%	1.88%	21,687 s

### 4.3 Rebar Localization Sub-system

In this subsection, some of the important details regarding rebar localization sub-system will be outlined. The rebar localization sub-system is the final component of the overall system proposed for rebar detection and localization in this research. Figure 8 presents the step-by-step transition and transformation of the input image from the output of the rebar detection sub-system, which is further processed in order to outline the specific region in which the rebar is present. The main goal within this sub-system is to ensure that the regions in the GPR B-scan images containing the rebar profiles can

be effectively highlighted, which can allow for the assessment of different rebar within the bridges. The automation of the rebar localization process can allow the bridge inspection personnel to examine the structural health of individual rebars within bridges.

It can be seen that image segmentation is performed with the help of K-mean clustering algorithm, which allows the segmentation of the different regions based on the varying color intensities. K-means clustering is an unsupervised learning-based algorithm, which separates image regions based on the level of color variations into different clusters [30]. As, it can be seen in Fig. 8, there are considerable variations between the foreground and background regions in rebar images. This particular aspect is leveraged to separate out the different image regions using the Image Thresholding technique, which transforms the image from RGB channels with varying color intensities to a single-channel-based binary image. In this manner, the essential foreground regions are highlighted in images, along with noise and high-intensity regions from the background regions. In order to ensure the ROI only contain regions with rebar profile hyperbolic signatures, the different morphological operations (e.g. opening, closing) are used to separate the foreground regions from the noise artefacts and background regions.



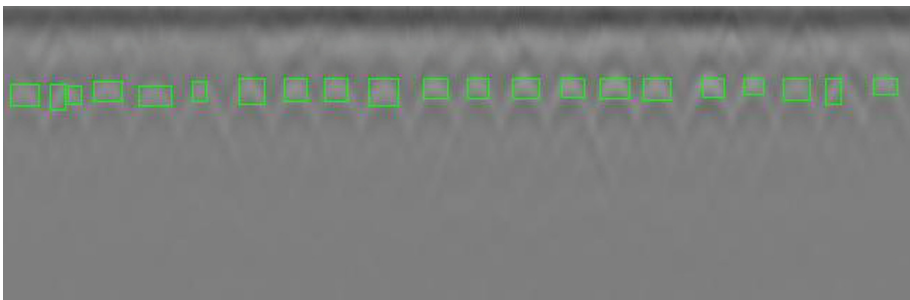
**Fig. 8.** Results for the different processes in the rebar localization sub-system

Table 4 outlines the overall performance of rebar localization sub-system in terms of accuracy and precision. The performance of the proposed rebar localization sub-system was evaluated on images with single and multiple rebar signatures. It can be seen from Table 4 that the overall accuracy for single rebar images is higher than for B-scan images containing multiple rebar signatures. For images with multiple rebar profiles, the sliding window-based approach was used to highlight different rebars within B-scan images. The overall accuracy of the rebar localization sub-system is at par with the different rebar localization systems developed in the previous studies [12, 19, 24]. A number of factors can affect the overall accuracy of localization of rebars in the B-scan images, such as high-level of noise artefacts in images, presence of multiple wave reflections, overlapping rebar signatures in B-scan images for multiple rebars, use of construction materials with varying properties (e.g. density, permittivity) and presence of non-rebar underground objects (e.g. pipes, utility lines, void spaces and underground metal objects) that exhibit similar hyperbolic signatures.

**Table 4.** Summary of results for Rebar Localization on dataset 1 and 2

Dataset	Single rebar localization		Multiple rebar localization	
	Accurate localization	Inaccurate localization	Accurate localization	Inaccurate localization
Dataset 1	1,426	73	854	64
Dataset 2	1,299	45	869	76
Total (%)	2,725 (95.85%)	118 (4.15%)	1,723 (92.49%)	140 (7.51%)
Total accuracy	94.52%		Total precision	95.18%

Figures 9 and 10 outline the results of rebar localization sub-system on a segment of B-Scan image obtained from dataset 1 and 2 respectively. It can be seen in Fig. 10 that the proposed system for rebar localization should be able to differentiate between actual rebar profiles and shadow effects, which can be seen in the lower portion of Fig. 10. It can also be observed that these shadow effects are much less pronounced in Fig. 9. Some of the examples of positive and negative results for rebar localization have been provided in Fig. 11.



**Fig. 9.** Results for the rebar localization on a segment of B-Scan image from dataset 1

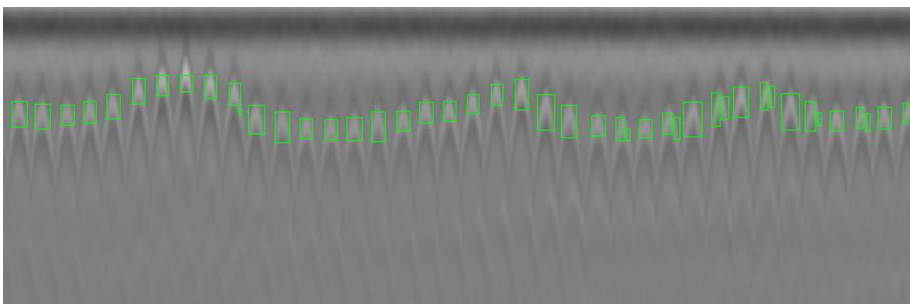


**Fig. 10.** Results for the rebar localization on a segment of B-Scan image from dataset 2

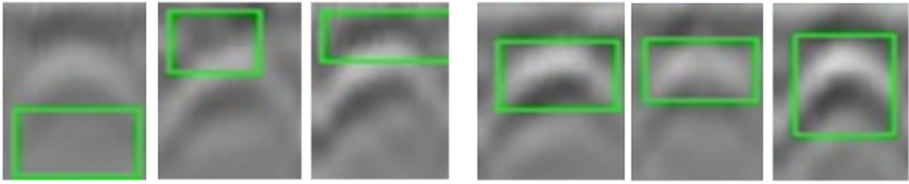


**Fig. 11.** Examples of negative (first three samples) and positive results for rebar localization

## 5 Conclusion

In this paper, a novel method for rebar detection has been developed, which utilizes the Deep Learning-based ResNet-50 architecture to train the system to differentiate between rebar and non-rebar images. At the same time, a novel method for rebar localization has also been presented, which uses image processing functions and bounding-box-based approach to outline the location of rebar within the B-scan images. The performance of the rebar detection and rebar localization sub-systems is comparable to some of the relevant state-of-the-art systems developed in the recent past [9, 12, 20, 24]. It can be concluded that this study has revealed compelling results, which warrant further investigation towards the usage of Deep Learning-based architectures to address the research problems related to NDE in general as well as rebar detection and localization in particular. Future comparative studies may provide insight into performance of different Deep Learning-based frameworks for the purpose of system development for rebar detection and localization. At the same time, additional data from different bridges can facilitate the assessment of the overall system performance and robustness due to varying *internal properties* (e.g. length and width of bridges, construction materials used, depth of rebar, total number of rebar used) and *external conditions* (e.g. levels of concrete delamination, rebar corrosion, weather conditions).

**Acknowledgment.** Financial support for this INSPIRE UTC project is provided by the U.S. Department of Transportation, Office of the Assistant Secretary for Research and Technology (USDOT/OST-R) under Grant No. 69A3551747126 through INSPIRE University Transportation Center (<http://inspire-utc.mst.edu>) at Missouri University of Science and Technology. The views, opinions, findings and conclusions reflected in this publication are solely those of the authors and do not represent the official policy or position of the USDOT/OST-R, or any State or other entity.

## References

1. Penn, A.: The deadliest bridge collapses in the US in the last 50 years. CNN, 15 March 2018
2. Kirk, R.S., Mallett, W.J.: Highway Bridge Conditions: Issues for Congress. US Congressional Research Service, Washington, D.C. (2013)
3. Wright, L., Chinowsky, P., Strzepek, K., et al.: Estimated effect of climate change on flood vulnerability of US bridges. *Mitig. Adapt. Strat. Glob. Change* **17**(8), 939–955 (2012)

4. Briaud, J.-L., Brandimarte, L., Wang, J., D'Odorico, P.: Probability of scour depth exceedance owing to hydrologic uncertainty. *Georisk* **1**(2), 77–88 (2014)
5. US Department of Transportation Report: 2015 Status of the Nation's Highways, Bridges, and Transit: Conditions and Performance, Pub. No: FHWA-PL-17-001. US Department of Transportation, Washington, DC (2015)
6. La, H.M., Gucunski, N., Dana, K.J., Kee, S.-H.: Development of an autonomous bridge deck inspection robotic system. *J. Field Robot.* **34**, 1489–1504 (2017)
7. DeVault, J.E.: Robotic system for underwater inspection of bridge piers. *IEEE Instrum. Meas. Mag.* **3**(3), 32–37 (2000)
8. Al-Nuaimy, W., Huang, Y., et al.: Automatic detection of buried utilities and solid objects with GPR using neural networks and pattern recognition. *J. Appl. Geophys.* **43**(2), 157–165 (2000)
9. Gibb, S., La, H.M., Le, T., Nguyen, L., Schmid, R., Pham, H.: Nondestructive evaluation sensor fusion with autonomous robotic system for civil infrastructure inspection. *J. Field Robot.* **35**, 988–1004 (2018)
10. Diamanti, N., Redman, N.: Field observations and numerical models of GPR response from vertical pavement cracks. *J. Appl. Geophys.* **81**, 106–116 (2012)
11. Gucunski, N., Kee, S.-H., La, H.M., Basily, B., Maher, A.: Delamination and concrete quality assessment of concrete bridge decks using a fully autonomous RABIT platform. *Struct. Monit. Maintenance* **2**(1), 19–34 (2015)
12. Kaur, P., Dana, K.J., Romero, F.A., Gucunski, N.: Automated GPR rebar analysis for robotic bridge deck evaluation. *IEEE Trans. Cybern.* **46**(10), 2265–2276 (2016)
13. La, H.M., Lim, R.S., Du, J., Zhang, S., Yan, G., Sheng, W.: Development of a small-scale research platform for intelligent transportation systems. *IEEE Trans. Intell. Transp. Syst.* **13**(4), 1753–1762 (2012)
14. La, H.M., Gucunski, N., Kee, S.-H., Nguyen, L.V.: Data analysis and visualization for the bridge deck inspection and evaluation robotic system. *J. Visual. Eng.* **3**(6), 1–16 (2015)
15. Mazzeo, B.A., Larsen, J., McElderry, J., Guthrie, W.S.: Rapid multichannel impact-echo scanning of concrete bridge decks from a continuously moving platform. In: *Proceedings of 43rd Annual Review of Progress in Quantitative Nondestructive Evaluation*, vol. 1806, pp. 1–6 (2017)
16. Wang, Z.W., Zhou, M., Slabaugh, G.G., Zhai, J., Fang, T.: Automatic detection of bridge deck condition from ground penetrating radar images. *IEEE TASE* **8**(3), 633–640 (2011)
17. Gamba, P., Lossani, S.: Neural detection of pipe signatures in ground penetrating radar images. *IEEE Trans. Geosci. Remote Sens.* **38**(2), 790–797 (2000)
18. Protopapadakis, E., Doulamis, N.: Image based approaches for tunnels' defects recognition via robotic inspectors. In: *Bebis, George, et al. (eds.) ISVC 2015. LNCS*, vol. 9474, pp. 706–716. Springer, Cham (2015). [https://doi.org/10.1007/978-3-319-27857-5\\_63](https://doi.org/10.1007/978-3-319-27857-5_63)
19. Gibb, S., La, H.M.: Automated rebar detection for ground-penetrating radar. In: *Bebis, George, et al. (eds.) ISVC 2016. LNCS*, vol. 10072, pp. 815–824. Springer, Cham (2016). [https://doi.org/10.1007/978-3-319-50835-1\\_73](https://doi.org/10.1007/978-3-319-50835-1_73)
20. Ahmed, H., La, H.M., Gucunski, N.: Rebar detection using Ground Penetrating Radar with state-of-the-art Convolutional Neural Networks. In: *Proceedings of 9th SHMII*, St. Louis, Missouri, 4–7 August 2019
21. La, H.M., Gucunski, N., Kee, S.H., Yi, J., Senlet, T., Nguyen, L.: Autonomous robotic system for bridge deck data collection and analysis. In: *Proceedings of IEEE/RSJ International Conference on Intelligent Robots and Systems (IROS)*, Chicago, IL, USA, 14–18 September 2014
22. Lim, R.S., La, H.M., Sheng, W.: A robotic crack inspection and mapping system for bridge deck maintenance. *IEEE Trans. Autom. Sci. Eng.* **11**(2), 367–378 (2014)

23. La, H.M., Lim, R.S., Basily, B., Gucunski, N., Yi, J., Maher, A., Romero, F.A., Parvardeh, H.: Mechatronic and control systems design for an autonomous robotic system for high-efficiency bridge deck inspection and evaluation. *IEEE Trans. Mechatron.* **18**(6), 1655–1664 (2013)
24. Dinh, K., Gucunski, N., Duong, T.H.: An algorithm for automatic localization and detection of rebars from GPR data of concrete bridge decks. *Autom. Constr.* **89**, 292–298 (2018)
25. Yu, L., Chen, H., Dou, Q., Qin, J., Heng, P.-H.: Automated melanoma recognition in dermoscopy images via very deep residual networks. *IEEE Trans. Med. Imaging* **36**(4), 994–1015 (2017)
26. Zhang, K., Sun, M., Han, T.X., Yuan, X., Guo, L., Liu, T.: Residual networks of residual networks: multilevel residual networks. *IEEE TCSVT* **28**(6), 1303–1314 (2018)
27. Kim, J.-H., Lee, J.-S.: Deep residual network with enhanced upscaling module for super-resolution. In: *IEEE CVPR*, pp. 913–922 (2018)
28. He, K., Zhang, X., Ren, S., Sun, J.: Deep Residual learning for image recognition. In: *Proceedings of ICCV*, pp. 770–778 (2016)
29. Chen, C.W., Luo, J., Parker, K.J.: Image segmentation via adaptive K-mean clustering and knowledge-based morphological operations with biomedical applications. *ITIP* **7**(12), 1673–1683 (1998)
30. Gonzales, R.C., Woods, R.E.: *Digital Image Processing*, 4th edn. Pearson, New York (2017)